

Cell Reports, Volume 24

Supplemental Information

Expanded Coverage of the 26S Proteasome

Conformational Landscape Reveals

Mechanisms of Peptidase Gating

Markus R. Eisele, Randi G. Reed, Till Rudack, Andreas Schweitzer, Florian Beck, Istvan Nagy, Günter Pfeifer, Jürgen M. Plitzko, Wolfgang Baumeister, Robert J. Tomko Jr., and Eri Sakata

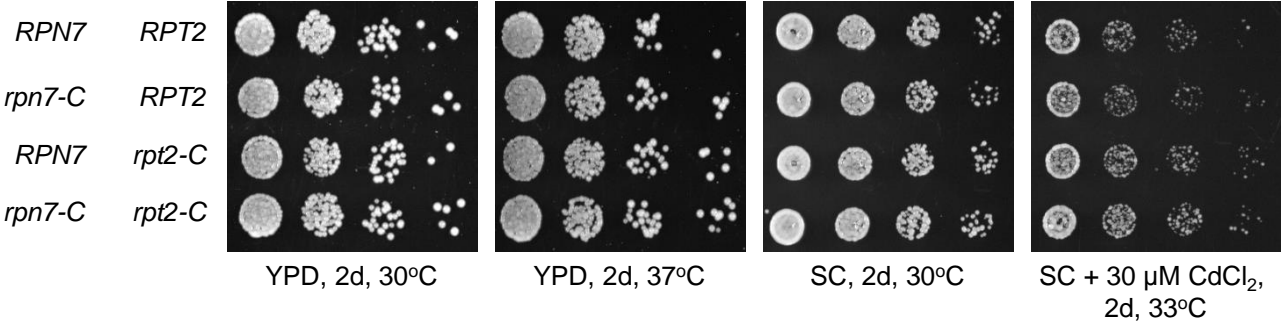
Table S1 related to Main Figures 1-7: Yeast strains used in this study.

Name	Genotype
RTY1	<i>MATa his3-Δ200 leu2-3,112 ura3-52 lys2-801 trp1-1</i> (alias MHY500)
RTY432	<i>MATa his3-Δ200 leu2-3,112 ura3-52 lys2-801 trp1-1 RPN5-6xGly-3xFLAG:hphMX4 rpt3Δ::HIS3</i> [YCplac33-RPT3]
RTY1168	<i>MATa his3-Δ200 leu2-3,112 ura3-52 lys2-801 trp1-1 rpt1Δ::HIS3</i> [pFL44-RPT1]
RTY1171	<i>MATa his3-Δ200 leu2-3,112 ura3-52 lys2-801 trp1-1 rpt4Δ::HIS3</i> [YCplac33-RPT4]
RTY1173	<i>MATa his3-Δ200 leu2-3,112 ura3-52 lys2-801 trp1-1 rpt6Δ::HIS3</i> [YCplac33-RPT6]
RTY1179	<i>MATa his3-Δ200 leu2-3,112 ura3-52 lys2-801 trp1-1 rpt6-Δ1:natMX4</i>
RTY1301	<i>MATa his3-Δ200 leu2-3,112 ura3-52 lys2-801 trp1-1 rpn6Δ::natMX4 rpt6Δ::HIS3</i> [pRS316-RPN6; YCplac33-RPT6]
RTY1321	<i>MATa his3-Δ200 leu2-3,112 ura3-52 lys2-801 trp1-1 rpt2Δ::HIS3</i> [pRS316-RPT2]
RTY1372	<i>MATa his3-Δ200 leu2-3,112 ura3-52 lys2-801 trp1-1 rpn7Δ::natMX4 rpt2Δ::HIS3</i> [pRS316-RPN7; pRS316-RPT2]
RTY1504	<i>MATa his3-Δ200 leu2-3,112 ura3-52 lys2-801 trp1-1 rpt3Δ::HIS3</i> [YCplac33-RPT3]
RTY1506	<i>MATa his3-Δ200 leu2-3,112 ura3-52 lys2-801 trp1-1 rpt5Δ::HIS3</i> [YCplac33-RPT5]
RTY1664	<i>MATa his3-Δ200 leu2-3,112 ura3-52 lys2-801 trp1-1 rpt1-Δ1:kanMX6</i>
RTY2013	<i>MATa his3-Δ200 leu2-3,112 ura3-52 lys2-801 trp1-1 RPN5-6xGly-3xFLAG:hphMX4 rpt6Δ::HIS3</i> [YCplac33-RPT6]
RTY2033	<i>MATa his3-Δ200 leu2-3,112 ura3-52 lys2-801 trp1-1 RPN5-6xGly-3xFLAG:hphMX4 rpt2Δ::HIS3</i> [pRS316-RPT2]
RTY2091	<i>MATa his3-Δ200 leu2-3,112 ura3-52 lys2-801 trp1-1 RPN7(D123C)-6xGly-V5:kanMX6</i>
RTY2099	<i>MATa his3-Δ200 leu2-3,112 ura3-52 lys2-801 trp1-1 RPT2(R407C):natMX4</i>
RTY2112	<i>MATa his3-Δ200 leu2-3,112 ura3-52 lys2-801 trp1-1 RPN7(D123C)-6xGly-V5:kanMX6 RPT2(R407C):natMX4</i>
RTY2123	<i>MATa his3-Δ200 leu2-3,112 ura3-52 lys2-801 trp1-1 rpt1-Δ1:kanMX6 rpt6-Δ1:natMX4</i>
RTY2166	<i>MATa his3-Δ200 leu2-3,112 ura3-52 lys2-801 trp1-1 pre8Δ::HIS3 pre9Δ::natMX4</i> [pRS316-PRE8]
RTY2135	<i>MATa his3-Δ200 leu2-3,112 ura3-52 lys2-801 trp1-1 RPN7(D123C)-6xGly-V5:kanMX6 RPT2(R407C):natMX4 rpt3Δ::HIS3</i> [YCplac33-RPT3]
RTY2137	<i>MATa his3-Δ200 leu2-3,112 ura3-52 lys2-801 trp1-1 RPN7(D123C)-6xGly-V5:kanMX6 RPT2(R407C):natMX4 rpt6Δ::HIS3</i> [YCplac33-RPT6]
YY540	<i>MATa ade2-1, ura3-1, his3-11, trp1-1, leu2-3,112, can1-100, rpn11::RPN11- 3xFLAG-CYC1term-HIS3</i>

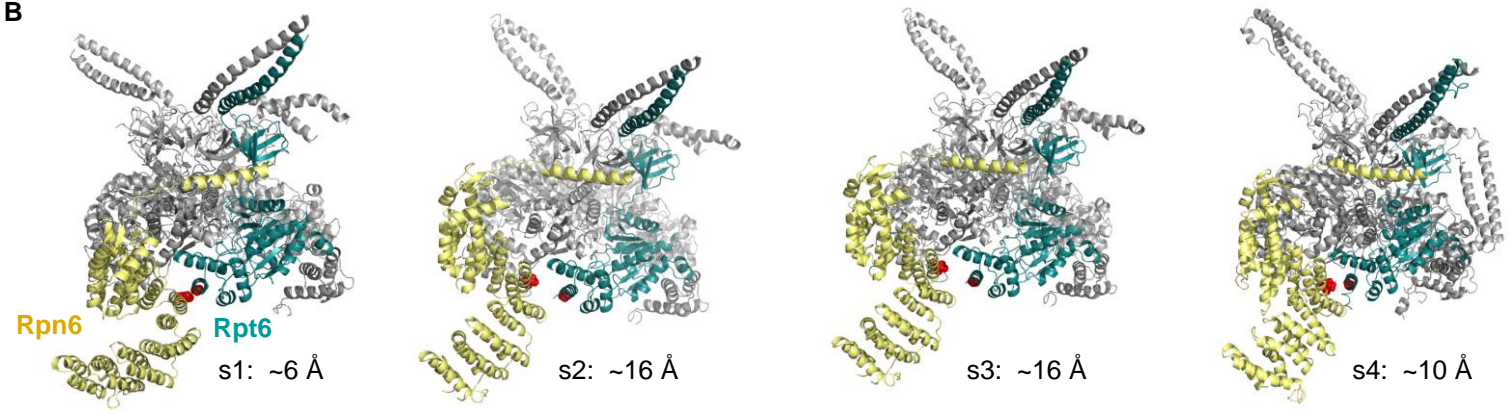
Table S2 related to Main Figures 1-7: Plasmids used in this study.

Plasmid	Genotype	Source
pRT357	pRS314- <i>RPT1</i>	This study
pRT364	YCplac111- <i>RPT3</i>	This study
pRT702	YCplac111- <i>RPT2</i>	This study
pRT1122	pET42b-6His-Cys-rpn12(C23S,D265A)	(Tomko et al., 2015)
pRT1408	pRS315- <i>RPT5</i>	This study
pRT1409	pRS314- <i>rpt1(E310Q)</i>	This study
pRT1410	YCplac111- <i>rpt2(E283Q)</i>	This study
pRT1411	YCplac111- <i>rpt3(E273Q)</i>	This study
pRT1413	pRS315- <i>rpt5(E282Q)</i>	This study
pRT1425	pRS314-HA- <i>RPN6</i>	This study
pRT1496	YCplac111- <i>RPT6</i>	This study
pRT1497	YCplac111- <i>rpt6(E249Q)</i>	This study
pRT1528	YCplac111- <i>RPT4</i>	This study
pRT1529	YCplac111- <i>rpt4(E283Q)</i>	This study
pRT1780	pRS314-HA- <i>RPN6(T203C)</i>	This study
pRT1783	YCplac111- <i>RPT2(R407C)</i>	This study
pRT1784	YCplac111- <i>RPT6(G387C)</i>	This study
pRT1834	YCplac111- <i>rpt2(E283Q, R407C)</i>	This study
pES1	pET28a-5Ub-DHFR-UR-His	This study

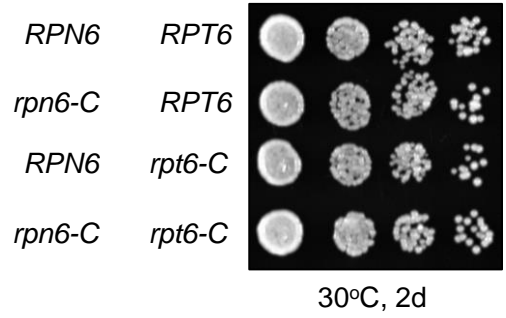
A



B



C



D

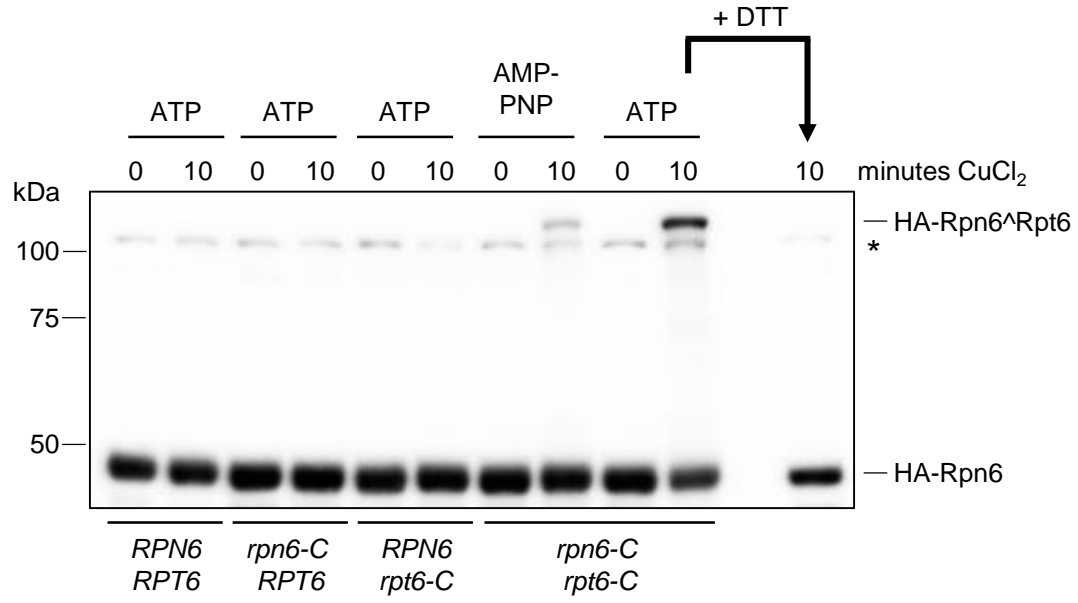


Figure S1

Figure S1 related to Figure 1. *A*, Cysteine substitutions do not impact cell health. The strains shown were plated as serial dilutions on YPD, SC, or SC+ 30 μ M CdCl₂ plates and incubated at the temperatures shown. *B*, Rpn6-T203 and Rpt6-G387 serve as an alternative conformational reporter. Rpn6 is shown in gold, Rpt6 in blue, and the other five Rpt subunits are shown in grey. All other subunits are omitted for clarity. The T203 and G387C residues are shown as red spheres, and the distances between their α carbons is listed in Angstroms. *C*, No obvious growth impairment in cells harboring the T203C and G387C substitutions. Serial dilutions were performed as in (*A*) above. *D*, Disulfide crosslinking of Rpn6 and Rpt6 is dependent upon engineered cysteines and impacted by nucleotide. Crosslinking was induced in whole cell extracts (WCE) prepared in the presence of 2 mM of the indicated nucleotide with CuCl₂ for ten minutes. Proteins were resolved by non-denaturing SDS-PAGE and examined by anti-HA (Rpn6) immunoblotting. For the last lane, the WCE was incubated with 10 mM DTT for 10 minutes prior to gel loading.

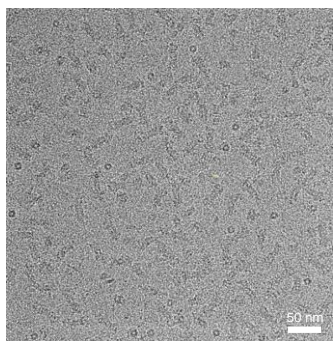
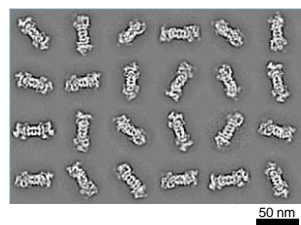
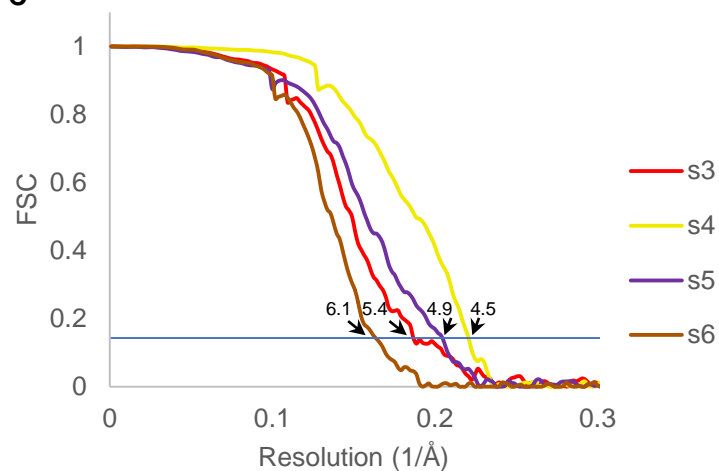
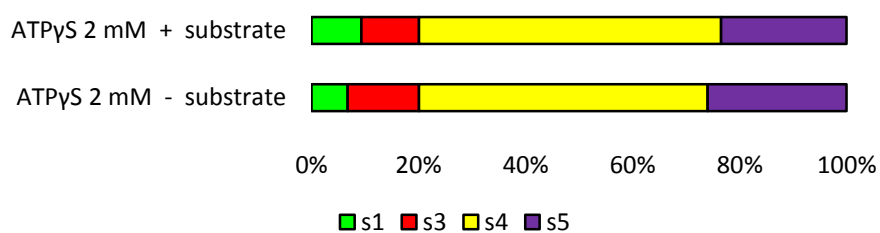
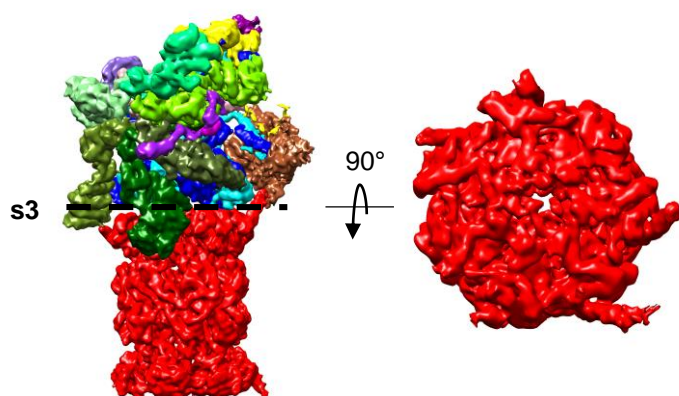
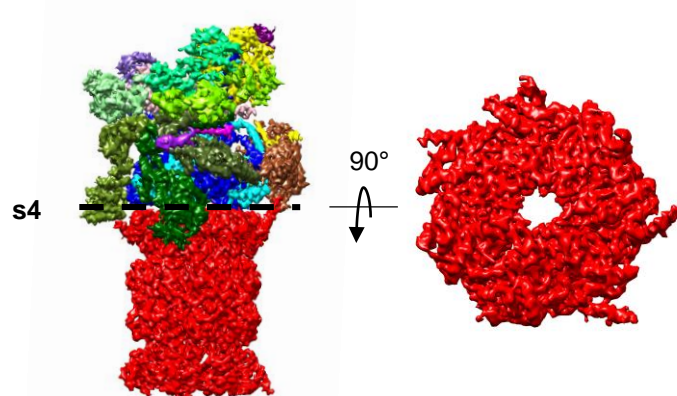
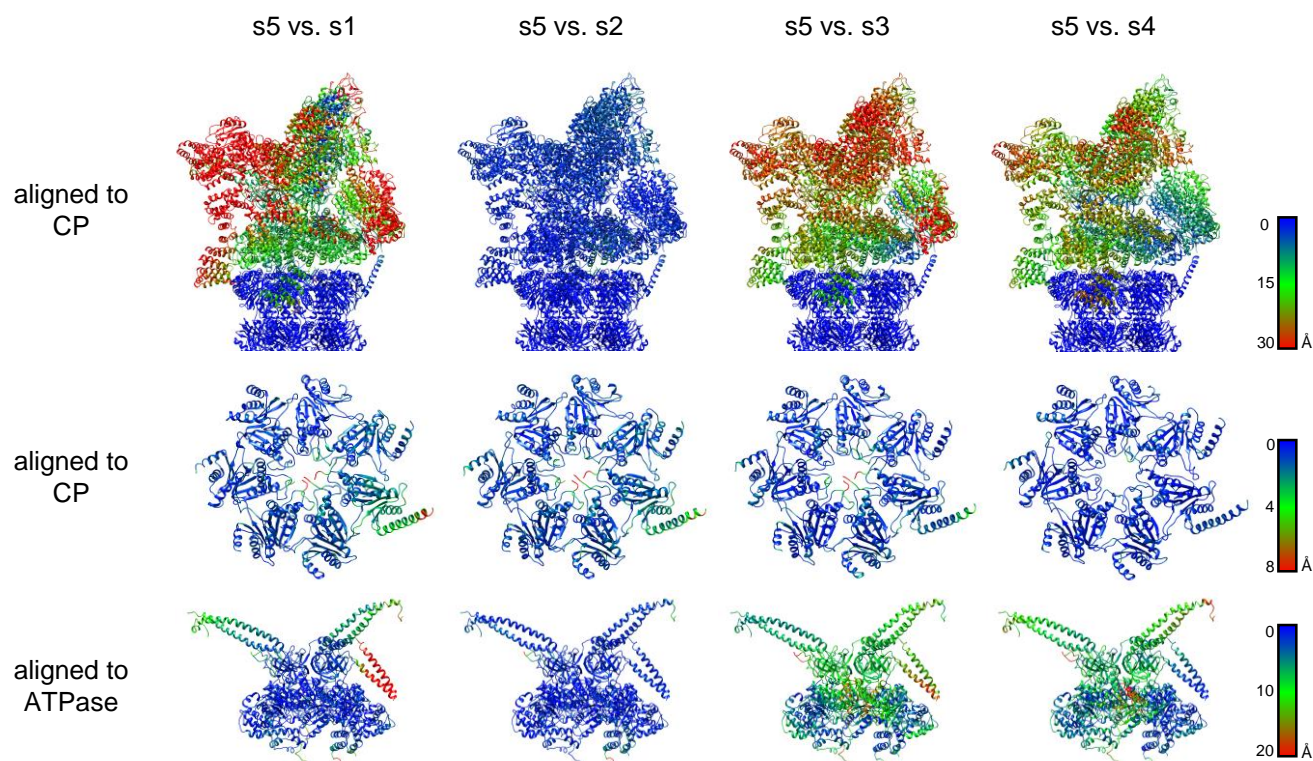
A**B****C****D****E****F****G****H****Figure S2**

Figure S2 related to Figure 2. *A*, Double capped particles are predominantly visible on a typical micrograph. *B*, Particles were 2D sorted and only suitable reference-free 2D class averages were used for further 3D analysis. *C*, Combined particles of each state resulted in a resolution of 4.5 Å for s4, 4.9 Å for s5, 5.4 Å for s3 and 6.1 Å for s6 on the basis of the gold-standard FSC criterion ($FSC_{0.143}$). *D*, Schematic of linear ubiquitinated DHFR with an unstructured region at the C-terminus. *E*, State distribution of classified 2 mM ATPγS data set with and without model substrate. *F* and *G*, Cryo-EM reconstruction of classified s3 particles (*F*) and s4 particles (*G*). The 26S proteasome is colored according to Fig 2B. A clear density is visible in the center of the 20S in the s3 state and no density is visible in the s4 state. *H*, Residue-wise RMSD of the whole 26S proteasome, the 20S gate and the AAA+ ATPase (in Å) between the s5 vs. s1 state (left), s5 vs. s2 state, s5 vs. s3 state and s5 vs. s4 state, aligned to the CP or to the ATPase. For the gate RMSD plots, the compared structures (either s1, s2, s3 or s4) are shown. In all other panels, the measured RMSD is plotted on the s5 structure.

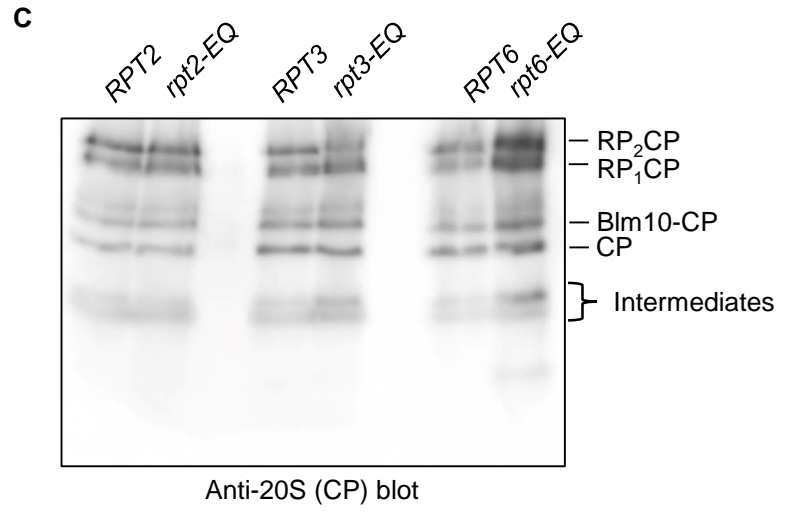
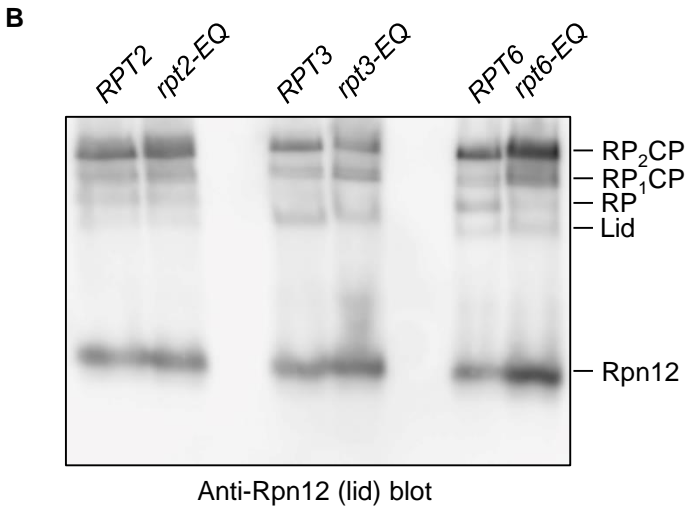
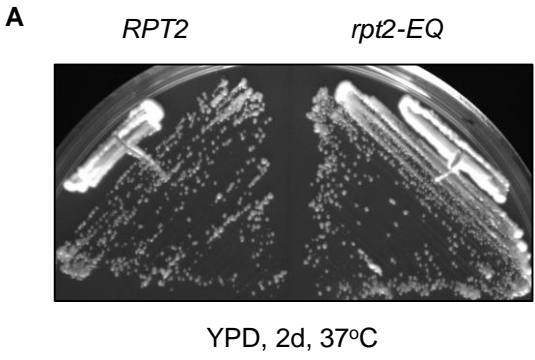


Figure S3

Figure S3 related to Figure 3. *A*, No evidence of temperature sensitivity in *rpt2-EQ* yeast. WT or *rpt2-EQ* yeast were struck on YPD, and incubated at 37°C for two days. *B* and *C*, Native gel immunoblot analysis of the indicated strains with anti-Rpn12 (*B*) or anti-20S (*C*) antibodies reveal no obvious structural defects. CP assembly intermediates are indicated with a bracket.

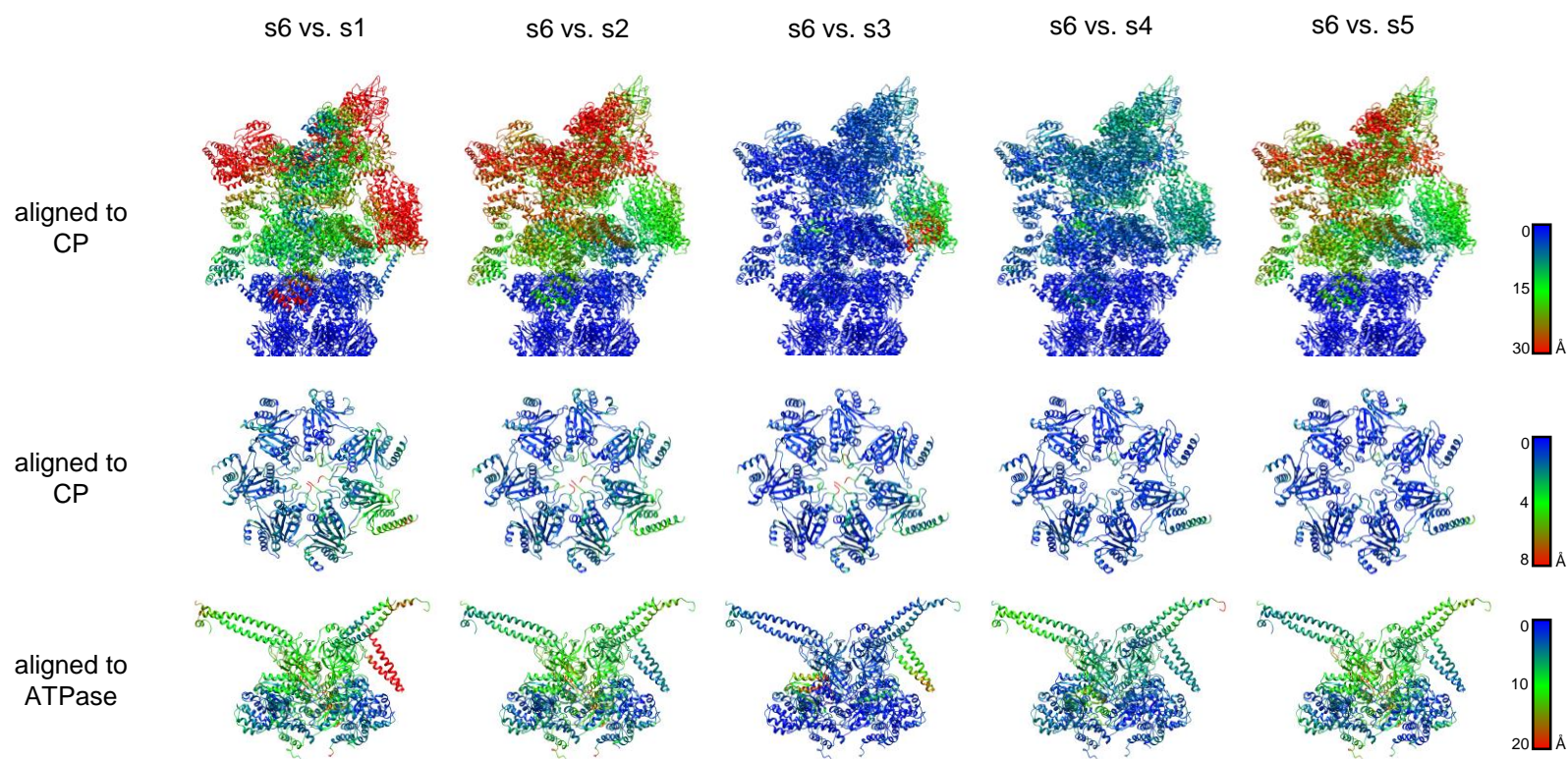


Figure S4

Figure S4 related to Figure 4. Residue-wise RMSD of the whole 26S proteasome, the 20S gate and the AAA+ ATPase (in Å) between the s6 vs. s1 state (left), s6 vs. s2 state, s6 vs. s3 state, s6 vs. s4 state and s6 vs. s5 state, aligned to the CP or to the ATPase. For the gate RMSD plots, the compared structures (either s1, s2, s3, s4 or s5) are shown. In all other panels, the RMSD is plotted on the s6 structure.

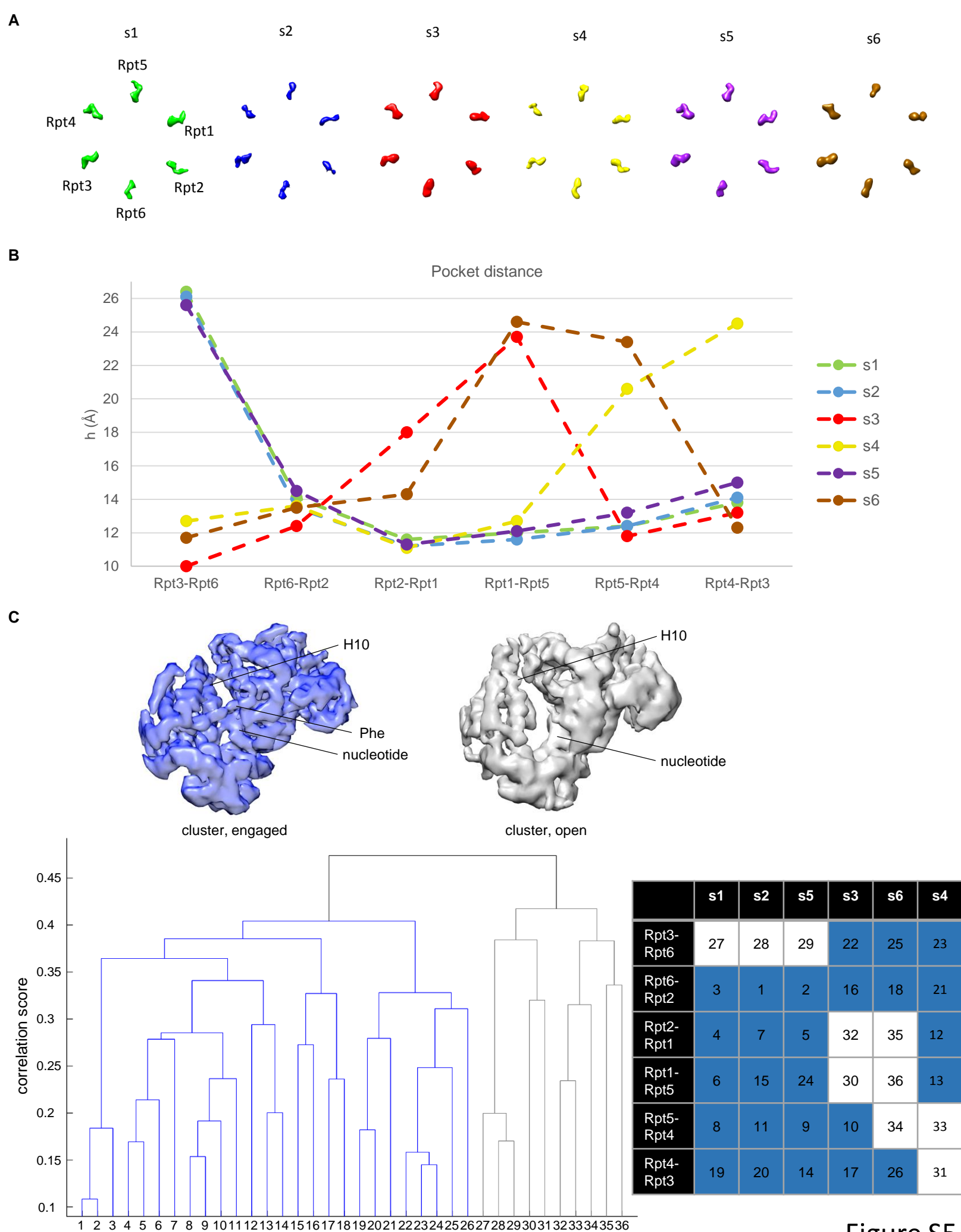
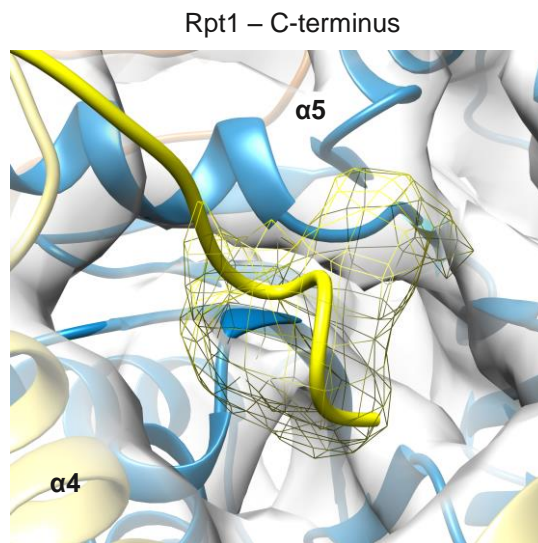
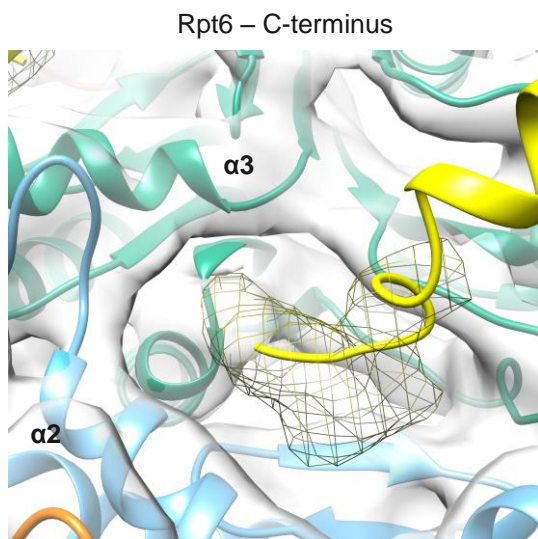


Figure S5

Figure S5 related to Figure 5. *A*, Comparison of nucleotide bound states in all six states. A simulated map of the AAA+ ring model without nucleotides was subtracted from the experimental map. EMD-3534 and EMD-3535 were used for s1 and s2 (Wehmer et al., 2017). The difference maps always show six nucleotides for each state. *B*, The state of the pocket is determined by measuring the distance between the end of the H10 helix of one Rpt subunit and the tip of H6 helix of the adjacent clockwise subunit. Color coding of each state would corresponds to the one in Figure 6A. *C*, Assessment of the EM density of the nucleotide binding pocket. Volumes of all Rpt subunits interfaces were aligned and hierarchically clustered by their similarity. The aligned densities were divided into two large clusters; the average of the blue class is assigned to the engaged conformation whereas the gray is assigned to the open conformation. An overview of the clustering results of the Rpt interface is shown in right lower panel. The numbers in the columns correspond to the numbering of the clustering on the left.

A**B**

hsRpt1	406	EKDFLEAVNKVIKSYAKFSATPRYMTYN
mmRpt1	448	EKDFLEAVNKVIKSYAKFSATPRYMTYN
drRpt1	406	EKDFLEAVNKVIKSYAKFSATPRYMTYN
xlRpt1	406	EKDFLEAVNKVIKSYAKFSATPRYMTYN
dmRpt1	406	EKDFLEAVKKVIKSYAKFSATPRYMTYN
atRpt1	399	EKDFLDVAVNKVIKGYQKFSATPKYMVYN
scRpt1	440	EKDFLKAVDKVISGYKKFSSISRYMQYN

C

hsRpt6	380	QEDFEMAVAKVMQKDSEKNMSIKKLWK
mmRpt6	380	QEDFEMAVAKVMQKDSEKNMSIKKLWK
drRpt6	380	QEDFEMAVAKVMQKDSEKNMSIKKLWK
xlRpt6	388	QEDFEMAVAKVMQKDSEKNMSIKKLWK
dmRpt6	379	QEDFEMAVAKVMQKDSEKNMSIKKLWK
atRpt6	378	QEDFEMAVSKVMKKEGESNMSIQRLWK
scRpt6	379	QEDFELAVGKVMNKNQETATISVAKLWK

Figure S6 related to Figure 6. *A*, EM densities of the C-termini of Rpt6 (left) and Rpt1 (right). The Rpt6 C-terminus is inserted between $\alpha 2$ and $\alpha 3$ and the Rpt1 C-terminus is inserted between $\alpha 4$ and $\alpha 5$. The EM density is depicted in gray. *B*, *C*, Boxshade alignments of the C-termini of Rpt1 (*B*) and Rpt6 (*C*) demonstrate high conservation of C-terminal amino acids.

Figure S7 related to Figure 7. *A*, Sequence alignment between *S. cerevisiae*, *H. sapiens*, *M. musculus*, *A. thaliana*, *D. melanogaster* and *M. jannaschii* of the first 60 amino acids of $\alpha 1$. The canonical clusters are marked in blue and the first α -helix in green. *B*, Sequence alignment of the canonical cluster amino acids of all seven α -subunits from *S. cerevisiae*, *H. sapiens*, *M. musculus*, *A. thaliana*, *D. melanogaster* and *M. jannaschii*. All canonical cluster amino acids but those from $\alpha 2$ of *M. jannaschii* are highly conserved, which explains the non-canonical cluster formed between $\alpha 1$ - $\alpha 2$. *C*, Example of YD-P-Y motif between $\alpha 6$ and $\alpha 7$ in the s5 state. The EM density is shown as mesh. *D*, The α subunit N-termini of $\alpha 2$, $\alpha 3$ and $\alpha 4$ undergo large movements between the closed and open gate conformations. Each N-terminus is depicted in a different color in the s5 state: $\alpha 1$ light orange, $\alpha 2$ light blue, $\alpha 3$ dark green, $\alpha 4$ yellow, $\alpha 5$ dark blue, $\alpha 6$ dark orange, $\alpha 7$ light pink. The localization of the N-terminal extensions of $\alpha 2$, $\alpha 3$ and $\alpha 4$ in the s2 state are visible in white. The structures of s2 and s5 were aligned onto the complete α chains of the CP. *E*, A proline movement of ~ 3.5 Å in $\alpha 2$ can be identified between all open and closed structures, here shown in states s5 (colored, light blue and dark green) and s2 (white). The C-terminus of Rpt6 inserts into the α subunit pocket between $\alpha 2$ and $\alpha 3$ in s3 (closed) and all open gate states, s4, s5 and s6. *F*, Model for ATP hydrolysis by 26S proteasome. In the absence of substrate, the proteasome is present in the ground state (s1), which represents the lowest energy conformation amongst the conformational states. When the proteasome is activated, most likely by substrate binding (Lu et al., 2015), it undergoes a conformational change from the ground state to a primed state (s2 or s5). The translocation of substrate may be triggered by ATP hydrolysis by one of the initiating ATPases coupled with ATP binding by Rpt6, leading the proteasome to an activated state (s3, s4 and s6). ATP hydrolysis can occur in either the lowermost engaged and most likely ATP-bound subunit, as was suggested for Yme1 (Puchades et al., 2017), or the highest engaged subunit (Martin et al., 2008), and continues around the ring. ATP hydrolysis causes a major conformational change in the neighboring subunits, leading to a new nucleotide-pocket configuration and to the next proteasome state of the hydrolysis cycle. Additional states may exist (s7, s8, s9). It is probable that the cycle continues until substrate translocation is completed. The cycle could include reversion to s2, s5, or s1.